

Asymptotic characteristics of decay channels of light nuclei states in the ab initio approach

D. M. Rodkin^{a,*}, Yu. M. Tchuvil'sky^{a,b}

^a*Dukhov Research Institute for Automatics, 127055, Moscow, Russia*

^b*Skobeltsyn Institute of Nuclear Physics, Lomonosov Moscow State University, 119991 Moscow, Russia*

Abstract

A new convenient method for precise theoretical calculations of quantities of traditional theory of nuclear reactions such as widths of resonances (including sub-threshold), and asymptotic normalization coefficients is proposed. This method may be considered as a step on the road to full theoretical ab initio description of light nuclei spectroscopic data. As an illustration of this method the computational results for all relevant two-body channels for all known and some theoretically predicted states of ${}^7\text{Li}$ nucleus are shown. Well-proven on a large amount of data Daejeon16 potential was used in the calculations. The most part of the results turn out to be in a good agreement with the experimental data contained in spectroscopic tables.

Keywords: nuclear structure, light nuclei, ab initio computation, decay channels

Modern high-precision methods for describing light nuclei properties and reactions induced by light nuclei collisions are advancing nowadays. These methods are based on new possibilities provided by modern high-performance supercomputers. An important role among the methods describing light nuclei structure belong to various ab initio methods, such as different versions of No-Core Shell Model (NCSM) [1, 2, 3, 4, 5], Gamov Shell Model (GSM) [6, 7], Green functions Monte Carlo method [8, 9, 10], the Coupled Cluster Method [11] and Lattice Effective Field Theory for Multi-nucleon Systems [12, 13, 14]. These methods are all based on realistic NN-, NNN-, etc. potentials. These potentials could be derived from Chiral Effective Field Theory [15, 16, 17] or from nucleon scattering data by the use of J -matrix inverse scattering method [18]. In the current paper we use Daejeon16 potential [15].

One of the most advanced ab initio methods for describing nuclear structure is No-Core Shell Model. This model is based on solving A -nucleon Schrödinger equation using realistic nucleon-nucleon potentials on the complete basis of totally antisymmetric A -nucleon wave functions up to the maximal total number of oscillator quanta N_{tot}^{max} . The size of this basis, for example, in widely used M-scheme reaches the value of about 10^{10} in the case that a modern supercomputer is employed. This method could be used for calculations of the binding energies, sizes, beta-decay lifetimes and electromagnetic observables characterizing ground, and excited states, as well as unstable resonances.

It should be mentioned that the range of distances where solutions of the Schrödinger equation are correctly described by NCSM A -nucleon wave functions (WFs) expands proportionally to $[N_{tot}^{max}]^{1/2}$. So this range is somewhat limited.

To adopt microscopic approaches for description of nuclear

reactions and the properties of nuclear resonance states it is necessary to describe various cluster channels. They are under investigation within traditional and modern models such as the Resonating Group Model (RGM) [19, 20], Algebraic Version of the RGM [21, 22], Generator Coordinate Method [23, 24], Microscopic Cluster Model [25, 26], THSR-approach [27], Antisymmetrized Molecular Dynamics [28]. For the most part these models are based on effective NN-potentials and used for calculations of specific highly clustered states.

Ab initio approaches focused on the discussed problem are also presented in the literature. Among them the methods which combine NCSM and RGM namely No-Core Shell Model / Resonating Group Model (NCSM/RGM) [29] and No-Core Shell Model with Continuum (NCSMC) [30, 31, 32, 33] seem to be the most versatile. Examples of a good description of the asymptotic characteristics of decay channels of the spectra of ${}^7\text{Be}$ and ${}^7\text{Li}$ are presented in [33]. As the NCSMC the Fermionic Molecular Dynamics (FMD) [34, 35, 36] offers in fact an ab initio approach focussed on the unified description of both bound states and continuum ones. Another approach – Cluster Channel Orthogonal Functions Method (CCOFM) – is also based on the employment of a basis combining NCSM and orthogonalized cluster-channel WFs [37, 38]. For the case of single-channel resonances some version of RGM [39] was put into use. To describe the resonance multi-neutron emission the SS-HORSE method was proposed [40]. Some nuclear resonances can be also studied with the use of mentioned above GSM. Anyway all these methods can be applied to a very limited number of nuclear states compare to the list of levels whose binding energies and electromagnetic properties are described by NCSM.

To make the mentioned above list of characteristics of nuclear states broader we proposed an approach [41] which is based on the calculations of the WFs of Hamiltonian eigenstates in the framework of conventional NCSM and projection of them onto the WFs of the cluster channels obtained in the framework

*I am corresponding author

Email address: rodkindm92@gmail.com (D. M. Rodkin)

of CCOFM [38]. In the current paper we present an advanced multi-channel version of the approach and the results of its application to the detail theoretical study of characteristics of ${}^7\text{Li}$ nucleus spectrum.

Let us demonstrate how translationally invariant A-nucleon WFs of arbitrary two-fragment decay channel with separation $A = A_1 + A_2$ are built in CCOFM. The useful feature of the procedure is that each function of this basis can be represented as a superposition of Slater determinants (SDs). To do that the technique of so-called cluster coefficients (CCs) is exploited.

The oscillator-basis terms of the cluster channel c_κ are expressed in the following form:

$$\Psi_{A,nl}^{c_\kappa} = \hat{A}\{\Psi_{A_1}^{[k_1]}\Psi_{A_2}^{[k_2]}\varphi_{nl}(\vec{\rho})\}_{J_c, J, M_J, T}, \quad (1)$$

where \hat{A} is the antisymmetrizer, $\Psi_{A_i}^{[k_i]}$ is a translationally invariant internal WF of the fragment labelled by a set of quantum numbers $\{k_i\}$; $\varphi_{nlm}(\vec{\rho})$ is the WF of the relative motion. The channel WF is labelled by the set of quantum numbers c_κ which includes $\{k_1\}, \{k_2\}, n, l, J_c, J, M_J, T$, where J is the total momentum and J_c is the channel spin. As it was mentioned above the function has to be represented as a linear combination of the SDs containing the one-nucleon WFs of the oscillator basis. For these purposes two-fragment WF in another representation

$$\Psi_{A,nlm}^{[k_1, k_2]} = \hat{A}\{\Psi_{A_1}^{[k_1]}\Psi_{A_2}^{[k_2]}\varphi_{nlm}(\vec{\rho})\}_{J_c, M_{J_c}, M_J, T} \quad (2)$$

is multiplied by the function of the center of mass (CM) zero vibrations $\Phi_{000}(\vec{R})$. Then the transformation of WFs caused by changing from $\vec{R}, \vec{\rho}$ to \vec{R}_1, \vec{R}_2 coordinates – different-mass Talmi-Moshinsky transformation is performed [42] and WF (2) takes the form

$$\Phi_{000}(\vec{R})\Psi_{A,nlm}^{[k_1, k_2]} = \sum_{N_i, L_i, M_i} \left\langle \begin{array}{c} 000 \\ nlm \end{array} \left| \begin{array}{c} N_1, L_1, M_1 \\ N_2, L_2, M_2 \end{array} \right. \right\rangle \quad (3)$$

$$\hat{A}\{\Phi_{N_1, L_1, M_1}^{A_1}(\vec{R}_1)\Psi_{A_1}^{[k_1]}\Phi_{N_2, L_2, M_2}^{A_2}(\vec{R}_2)\Psi_{A_2}^{[k_2]}\}_{J_c, M_{J_c}, M_J, T}.$$

The main procedure of the method is to transform internal WFs corresponding to each fragment multiplied by none-zero center of mass vibrations into a superposition of SDs

$$\Phi_{N_i, L_i, M_i}^{A_i}(\vec{R}_i)\Psi_{A_i}^{[k_i]} = \sum_k X_{N_i, L_i, M_i}^{A_i(k)} \Psi_{A_i(k)}^{SD}. \quad (4)$$

Quantity $X_{N_i, L_i, M_i}^{A_i(k)}$ is called a cluster coefficient (CC). Technique of these objects is presented in detail in [43]. There is a large number of methods elaborated for the calculations of CCs. The most general scheme is based on the method of the second quantization of the oscillator quanta. In this scheme the WF of the CM motion is presented as

$$\Phi_{N_i, L_i, M_i}^{A_i}(\vec{R}_i) = N_{N_i, L_i}(\hat{\mu}^\dagger)^{N_i - L_i} Y_{N_i, L_i}(\hat{\mu}^\dagger) \Phi_{000}^{A_i}(\vec{R}_i), \quad (5)$$

where $\hat{\mu}^\dagger$ is the creation operator of the oscillator quantum, and N_{N_i, L_i} is the norm constant. Thus the CC turns out to be reduced to a matrix element of the tensor operator expressed in terms of $\hat{\mu}^\dagger$:

$$\langle \Psi_{A_i(k)}^{SD} | \Phi_{N_i, L_i, M_i}^{A_i}(\vec{R}_i)\Psi_{A_i}^{[k_i]} \rangle = N_{N_i, L_i} \langle \Psi_{A_i(k)}^{SD} | (\hat{\mu}^\dagger)^{N_i - L_i} Y_{N_i, L_i}(\hat{\mu}^\dagger) | \Phi_{000}^{A_i}(\vec{R}_i)\Psi_{A_i}^{[k_i]} \rangle \quad (6)$$

A conventional relationship between the translationally invariant and an ordinary shell-model WFs

$$\Psi_{A_i}^{shell} = \Psi_{A_i}^{[k_i]} * \Phi_{000}^{A_i}(\vec{R}_i) \quad (7)$$

is used as a definition of the former one. The NCSM WFs of the fragments $\Psi_{A_i}^{shell}$ are involved in the calculations.

The last step is to construct $\Psi_{A,n}^{c_\kappa}$ basis wave functions for each channel c_κ (1) from a basis of $\Psi_{A,nlm}^{[k_1, k_2]}$ (2) by the use of ordinary Clebsh-Gordan coefficients.

It should be noted that WFs of cluster-channel terms (1) of one and the same channel c_κ characterized by the pair of internal functions $\Psi_{A_1}^{[k_1]}, \Psi_{A_2}^{[k_2]}$ and extra quantum numbers l, J_c, J, M_J, T are non-orthogonal. Creation of orthonormalized basis functions of channel c_κ is performed by the diagonalization of the exchange kernel

$$\|N_{nn'}\| = \langle \Psi_{A,n'}^{c_\kappa} | \Psi_{A,n}^{c_\kappa} \rangle = \langle \Psi_{A_1}^{[k_1]} \Psi_{A_2}^{[k_2]} \varphi_{nl}(\rho) | \hat{A}^2 | \Psi_{A_1}^{[k_1]} \Psi_{A_2}^{[k_2]} \varphi_{n'l}(\rho) \rangle. \quad (8)$$

The eigenvalues and eigenvectors of this exchange kernel are given by the expressions:

$$\varepsilon_{\kappa,k} = \langle \hat{A}\{\Psi_{A_1}^{[k_1]} \Psi_{A_2}^{[k_2]} f_l^k(\rho)\} | \hat{A}\{\Psi_{A_1}^{[k_1]} \Psi_{A_2}^{[k_2]} f_l^k(\rho)\} \rangle; \quad (9)$$

$$f_l^k(\rho) = \sum_n B_{nl}^k \varphi_{nl}(\rho). \quad (10)$$

As a result, the WF of the orthonormalized basis channel c_κ is represented in the form

$$\Psi_{A,kl}^{SD,c_\kappa} = \varepsilon_{\kappa,k}^{-1/2} | \hat{A}\{\Psi_{A_1}^{[k_1]} \Psi_{A_2}^{[k_2]} f_l^k(\rho)\} \rangle, \quad (11)$$

The cluster form factor (CFF) is a projection of the function of an initial A-nucleon state Ψ_A onto the WF of a particular channel c_κ . It describes the relative motion of subsystems and has the form

$$\begin{aligned} \Phi_A^{c_\kappa}(\rho) &= \sum_k \varepsilon_{\kappa,k}^{-1/2} \langle \Psi_A | \hat{A}\{\Psi_{A_1}^{[k_1]} \Psi_{A_2}^{[k_2]} f_l^k(\rho)\} \rangle f_l^k(\rho) \\ &= \sum_k \varepsilon_{\kappa,k}^{-1/2} \sum_{n,n'} B_{nl}^k B_{n'l}^k C_{AA_1 A_2}^{n'l} \varphi_{nl}(\rho) \end{aligned} \quad (12)$$

where

$$\begin{aligned} C_{AA_1 A_2}^{nl} &= \langle \hat{A}\{\Psi_{A_1}^{[k_1]} \Psi_{A_2}^{[k_2]} \varphi_{nl}(\rho)\} | \Psi_A \rangle = \\ &= \langle \Psi_{A,nl}^{SD,c_\kappa} | \Phi_{000}(\vec{R}) | \Psi_A \rangle = \langle \Psi_{A,nl}^{SD,c_\kappa} | \Psi_A^{SM} \rangle. \end{aligned} \quad (13)$$

is called the spectroscopic amplitude. A number of very diverse methods of its calculation depending on the masses of the initial nuclei and fragments were described in [43, 44, 45, 46]. The amplitude of the CFF is determined as

$$K_{AA_1 A_2}^{nl} = \sum_{k,n'} \varepsilon_{\kappa,k}^{-1/2} B_{nl}^k B_{n'l}^k C_{AA_1 A_2}^{n'l}. \quad (14)$$

The spectroscopic factor of this channel c_κ has the form

$$S_l^{c_\kappa} = \int |\Phi_A^{c_\kappa}(\rho)|^2 \rho^2 d\rho =$$

$$\sum_k \varepsilon_k^{-1} \sum_{mm'} C_{AA_1A_2}^{nl} C_{AA_1A_2}^{n'l'} B_{nl}^k B_{n'l'}^k. \quad (15)$$

The definitions of the CFF (13) and spectroscopic factor (15) are completely equivalent to those proposed in [47] (the so-called new spectroscopic factor and CFF). In contrast to the traditional definition, the new spectroscopic factor characterizes the total contribution of orthonormalized cluster components to the solution of the Schrödinger equation for A nucleons. Reasons for the necessity of its use to describe decays and reactions can be found in [48, 49]. In [50, 51], it was demonstrated that the correct definition eliminates a sharp contradiction between theoretical calculations of the cross sections for reactions of knockout and transfer of α clusters and experimental data.

Compared to the spectroscopic factor the CFF is a more informative characteristic because it allows its matching with the asymptotic WF of the relative motion in the range of validity of shell-model solution and thus determines the amplitude of the WF in the asymptotic region.

It is convenient to use the CFF for computing the widths of resonances and the asymptotic normalization coefficients (ANCs) of bound states, which in turn are used to calculate the cross sections of resonant and peripheral reactions respectively. The CFF in its new definition allows matching with the asymptotic WF at relatively small distances, where the nuclear interaction is negligibly weak, but exchange effects generated by the anti-symmetry of the total channel WF are still not negligibly small. This property is very important for dealing with NCSM WFs.

In this approach, a direct matching procedure is applied to calculate the ANCs of bound states and the widths of narrow resonances. For such resonances or, more precisely, for those of them whose small width is due to a low penetrability of the potential barrier, we used a very compact procedure proposed in [52]. This procedure is applicable because for such resonances there is sufficiently wide range of distances in which the nuclear attraction is already switched off and at the same time the potential barrier is high enough. At any inner point ρ_{in} of this area, the relationship between the regular and irregular solutions of the two-body Schrödinger equation in the WKB approximation has the form

$$F_l(\rho_{in})/G_l(\rho_{in}) = P_l(\rho_{in}) \ll 1 \quad (16)$$

where $P_l(\rho_{in})$ is the penetrability of the part of the potential barrier which is located between the point ρ_{in} and the outer turning point. The smallness of this penetrability is the condition of applicability of the approximation, where the contribution of the regular solution can be neglected. To determine the position of the matching point of the CFF and irregular WF in this range, we use the condition of equality of the logarithmic derivatives

$$\frac{d\Phi_A^{c_k}(\rho)/d\rho}{\Phi_A^{c_k}(\rho)} = \frac{dG_l(\rho)/d\rho}{G_l(\rho)}, \quad (17)$$

which determines the matching point ρ_m ; therefore, the decay width is given by the expression

$$\Gamma = \frac{\hbar^2}{\mu k} \left[\frac{\Phi_A^{c_k}(\rho_m)}{G_l(\rho_m)} \right]^2. \quad (18)$$

The matching of logarithmic derivatives is also used to determine the ANCs A^{c_k} . This value is defined as a ratio of the CFF and the Whittaker function $W_{-\eta, l+1/2}(2k\rho)$ in the range of distances where the nuclear interaction is already weak [53, 54]

$$A^{c_k} = \rho_m \Phi_A^{c_k}(\rho_m) / W_{-\eta, l+1/2}(2k\rho_m). \quad (19)$$

In several spectroscopic data tables [55] the decay widths of sub-threshold resonances are given. To establish a link with such data we calculate the decay widths of such a type by the use of the formulation given in [56]:

$$\Gamma_{subth}(E) = \frac{\hbar^2}{\mu_{ab}} k \rho_m P_l(E) \frac{W_{-\eta, l+1/2}^2(2k_0\rho_m)}{\rho_m} |A^{c_k}|^2 \quad (20)$$

where $k_0 = \sqrt{2\mu_{ab}c^2 E_{state}} / (\hbar c)$.

To make the list of the properties of the states of a certain nucleus complete large-width resonances are considered too. If the resonance is wide and so the penetrability $P_l(\rho_{in})$ (16) is not small the width of this resonance is calculated using the simple version of the conventional R-matrix theory:

$$\Gamma = \frac{\hbar^2}{\mu k_0} (F_l^2(\rho_m) + G_l^2(\rho_m))^{-1} (\Phi_A^{c_k}(\rho_m))^2. \quad (21)$$

Naturally the use of this version leads to reduction in accuracy of calculation results, but it should be noted that the accuracy of the data, concerning large-width resonances, extracted from various experiments is also very limited. Thus, together with calculations using NCSM model our method allows one to calculate simultaneously nearly all properties of ground and excited states of light nuclei.

The critical point of the approach is a correct representation of the form of the CFF at distances at which, first, the nuclear interaction is negligible and, second, the "memory" of the exchange effects remains exclusively in the exchange kernel matrix $\|N_{mm'}\|$. In this work the proposed approach is tested by computing of the asymptotic characteristics of all relevant two-body channels for all known and some theoretically predicted states of ${}^7\text{Li}$ nucleus together with the spectrum of this nuclide.

An important point is that the Daejeon16 potential [15] is used as a model of NN-interaction. It is built using the N3LO limitation for of Chiral Effective Field Theory [57] softened by Similarity Renormalization Group (SRG) transformation [58]. This potential is designed to calculate all kinds of characteristics of nuclei with the masses $A \leq 16$. starting from one and the same set of the parameters of NN-interaction. It was tested in the framework of broad calculations of the total binding energies, excitation energies, radii, moments of nuclear states and the electromagnetic reduced probabilities. These tests demonstrated that such characteristics are, in general, reproduced well. To calculate the WFs of the ${}^7\text{Li}$ nucleus, and its subsystems within the NCSM, we use the Bigstick shell-model code [59], which is convenient for multiprocessor computer clusters. The basis cutoff parameter $N_{tot}^{max} = 15$ was reached for the computation of the energies and WFs of the ${}^7\text{Li}$ nucleus states. The optimal oscillator parameter $\hbar\omega$ for the calculations with the realistic NN-potential Daejeon16 turns out to be 20.0 MeV.

Table 1: Amplitudes of the CFF $K_{AA_1A_2}^{n=1}$ of all nodal quantum numbers for the ground state of ${}^7\text{Li}$ and ${}^4\text{He}+{}^3\text{H}$ channel in various bases used to calculate WFs of initial nuclei and subsystems.

N_{tot}^{max}	N_{cl}^{max}	n=1	n=3	n=5	n=7
13	0	0.0	0.745	-0.419	0.262
	2	0.007	0.752	-0.435	0.271
	4	0.092	0.753	-0.440	0.0
15	0	0.0	0.729	-0.421	0.273
	2	0.006	0.736	-0.436	0.282
	4	0.090	0.737	-0.443	0.288

According to equations (18,19, 20, 21) the ANC's and decay widths of nuclear states depend on the value of channel form factor at the matching point. The coefficients (amplitudes) $K_{AA_1A_2}^{n=1}$ of its oscillator expansion for the ground state of ${}^7\text{Li}$ and ${}^4\text{He} + {}^3\text{H}$ channel are summarized in Tab. 1. The data presented in this table indicate that the dominant amplitudes of the CFF come down to their real values already for the basis cut-off parameter $N_{tot}^{max} = 13$ and the choice of the cutoff parameter N_{cl}^{max} of the bases of the cluster WFs weakly affects these quantities. The measure of the convergence can be defined as the total standard deviation of the amplitudes of the CFF in different calculation variants. If one excludes the case $N_{tot}^{max} = 13$ and $N_{cl}^{max} = 4$, where the dimension of the basis is insufficient to calculate the amplitude which is characterized by the nodal quantum number $n = 7$, this deviation becomes less than 1%. So the channel form factor doesn't depend noticeably on the accuracy of the subsystem description and the choice of nearly all combinations of subsystems cut off parameters is adequate.

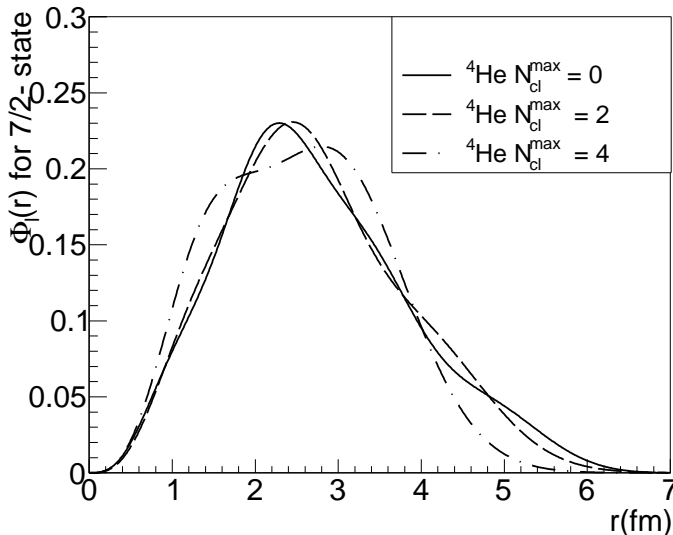


Figure 1: CFFs $\Phi_l(r)$ for $7/2_1^-$ state of ${}^7\text{Li}$ for ${}^4\text{He}+{}^3\text{H}$ channel as function of relative distance for different values of cutoff parameter N_{cl}^{max} of the cluster WF.

As another demonstration of the fact that CFF depends only slightly on the choice of the cutoff parameter N_{cl}^{max} , the CFFs

for $7/2_1^-$ state and ${}^4\text{He}+{}^3\text{H}$ channel are shown in Fig. 1.

For all low-lying resonances and bound states the channel form factors are matched with asymptotic solutions. As an example these asymptotic solutions are shown for $7/2_1^-$ state and ${}^4\text{He}+{}^3\text{H}$ channel in Fig. 2. For this state the condition $F_l(\rho_{in}) \ll G_l(\rho_{in})$ is exactly satisfied in fact. So the contribution of the regular solution can be neglected and one may determine the position of the matching point taking into account the irregular solution only.

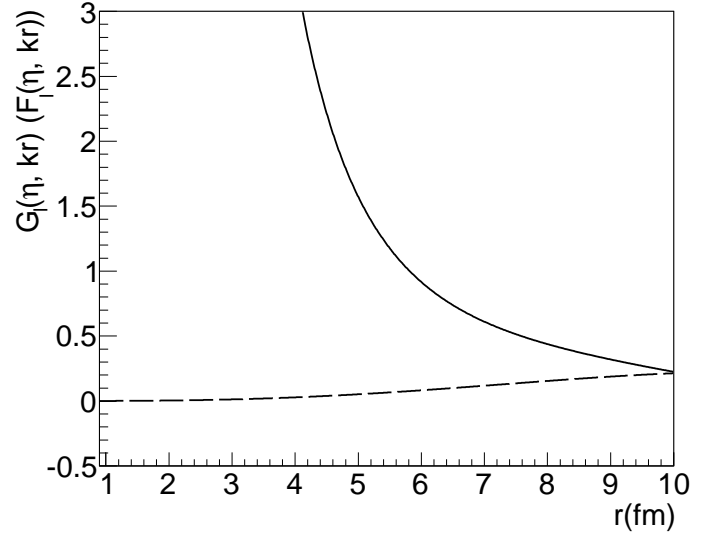


Figure 2: Asymptotic regular (dashed line) and irregular (solid line) solutions for $7/2_1^-$ state of ${}^7\text{Li}$ for ${}^4\text{He}+{}^3\text{H}$ channel.

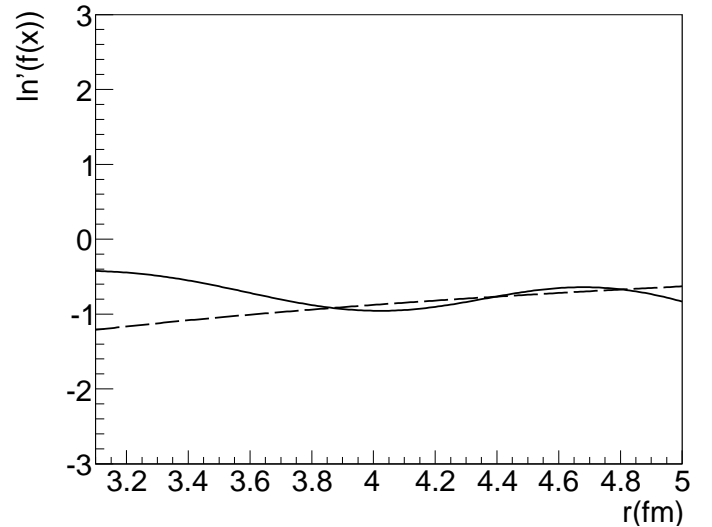


Figure 3: Logarithmic derivatives of CFF $\Phi_l(r)$ (solid line) and irregular asymptotic solution (dashed line) for $7/2_1^-$ state of ${}^7\text{Li}$ for ${}^4\text{He}+{}^3\text{H}$ channel.

Bearing in a mind mentioned above problems appearing in the NCSM calculations of WFs at large inter-fragment distances a reproducibility of the form of asymptotic WF by the CFF in this region turns out to be a key question. Fig.3 demonstrates a high quality of the reproducibility in the discussed example.

The ratios of the CFFs and the asymptotic WFs change weakly in the region of matching point (see below Fig. 5). Due to that the result of the matching procedure turn out to be tolerant to occasional deviation of the matching point in rather wide range of distances. Moreover this circumstance allows one to overcome difficulties which could occur in the case that a synthesis of the using projection procedure and the microscopic R-matrix theory [60] would be required.

As it is shown in Tabs. 2 – 4 the total binding energies of the lower levels of the ${}^7\text{Li}$ nucleus obtained in our calculations reproduce the measured values with accuracy conventionally considered satisfactory and are in good agreement with the NCSM calculations, which we received by us through personal communication with the authors of this potential. The energies of highly-excited states are reproduced with a lower accuracy especially for states with relatively small spin or positive parity. The insufficient dimension of the basis employed and, possibly, some features of the potential used are the causes of that. At the same time, the performed calculations demonstrate that the asymptotic characteristics of the channels under study are highly sensitive to the fragmentation energy. In particular, the ANC of $3/2^-$ state varies from 3.44 to 3.30 $\text{fm}^{-1/2}$ (by 3%) at replacement of the experimental energy $E_{exp.} = -2.467$ MeV by the computed value $E_{th.} = -2.529$ MeV, i.e. at the change in the energy by 62 keV. This difference for the $1/2^-$ state, the change is equal to 0.29 MeV in this example (it is a rare case when the excitation energy is poorly reproduced in our and all other calculations using great bases hence originated by features of the Daejeon16 potential itself), is 24%. The decay widths are even more sensitive to the fragmentation energy. Indeed, in the case of $7/2^-$ state a very small only 23 keV difference in resonance energy (in the case of replacement of the experimental energy 2.195 by the calculated one – 2.172 MeV) leads to 5% difference in decay width (from 65 keV to 62.2 keV). It is clear enough that modern ab initio computations cannot reproduce the fragmentation energy of the decay channels with the precision that required for the discussed purposes, therefore the calculations which are based on the experimental values of the decay energies are preferable. We follow that choice. Our calculation show that the coordinates of the matching point turn out to be rather stable and have a little impact on the results.

To complete the presentation of the methodical aspects of the proposed approach it is appropriate to compare them with the features of the approach designed in Ref. [33], where ${}^7\text{Li}$ and ${}^7\text{Be}$ asymptotic properties were studied with the use of NC-SMC model. As it was mentioned above, the NCSMC model is a well self-consistent ab initio approach to unified description of nuclear structure and reactions. It is focussed on the description of compound states of nuclei together with their real or virtual, nucleon or light cluster decay channels. A realistic NN-potential softened via the SRG transformation is used in the discussed paper. The value of the parameter of this transformation $\lambda_{SRG} = 2.15 \text{ fm}^{-1}$ has been chosen as the best that reproduces the experimental separation energies of nucleons and clusters in ${}^7\text{Be}$ and ${}^7\text{Li}$ nuclei. The NCSMC model allows one to compute ANCs of bound states and partial decay widths of resonances, both narrow and wide. At present the capability of

this approach are limited by one-channel problem and the mass of the light fragment $A \leq 3$. The approach presented in the current paper looks more simple and the mass of the light fragment is not a strong limitation. The asymptotic characteristics of all two-body decay channels of a certain state can be calculated simultaneously. The well-tested on the large basis of nuclear data Daejeon16 NN-potential is used in the approach. A possibility to involve into consideration experimental values of decay energies makes the approach more flexible. In a lot of examples this increases the quality of description of the spectroscopic data. That is why we believe that the developed approach extends the possibilities of ab initio methods to describe characteristics of various of nuclear states and their decay channels and makes the description more accurate in many cases. What about the correlation of the numerical results obtained by the discussed approaches one may conclude that the results presented in Ref. [33] and the results shown in the current paper below being different in particular examples can be generally qualified as good ones.

The results of the calculations of asymptotic characteristics of all relevant virtual and real decay channels (${}^4\text{He} + {}^3\text{H}$, ${}^6\text{Li} + n$, ${}^6\text{He} + p$, ${}^6\text{Li}(E^* = 3.562 \text{ MeV}, T = 1) + n$) for all known ${}^7\text{Li}$ and some theoretically predicted states are summarized in Tabs. 2 – 4.

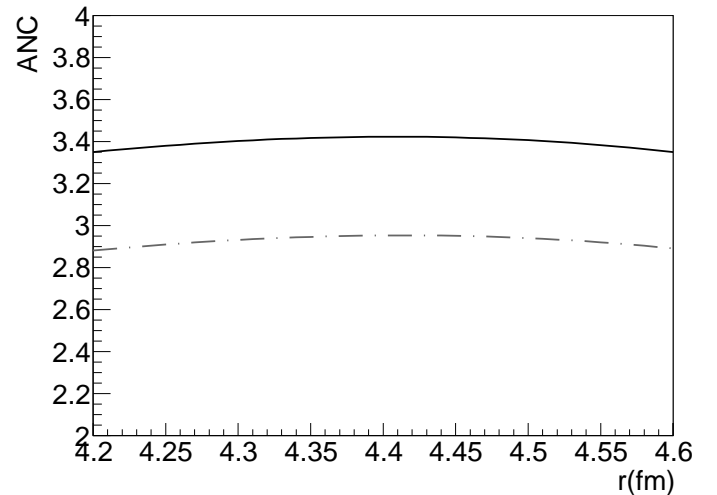


Figure 4: Asymptotic normalization coefficient in the region of matching point for the $3/2^-$ (solid line) and $1/2^-$ (dash-dotted line) states.

The matching points for $3/2^-$ and $1/2^-$ states for ${}^4\text{He} + {}^3\text{H}$ channel almost coincide. It is important that ratio (19) near their matching point hardly changes for both states, as seen in Fig. 4. This confirms once more the stability of the procedure used to calculate the ANCs. The results are also in a good agreement with the values extracted from experiments (see Tab. 2).

Table 2: Asymptotic characteristics of ${}^7\text{Li}$ for ${}^4\text{He}+{}^3\text{H}$ and ${}^6\text{Li}+n$ channels for bound negative parity states and high-excited positive parity state.

J^π, T	$E_{exp.}(E_{th.})$ MeV	$E_{\alpha+t}^{exp.}$ ($E_{\alpha+t}^{th.}$) MeV	$\Gamma_\alpha(\text{ANC})$ [61]	$\Gamma_\alpha(\text{ANC})$ th.	$E_n^{exp.}$ ($E_n^{th.}$) MeV	$\Gamma_n(\text{ANC})$ [55, 63]	$\Gamma_n(\text{ANC})$ th.
$3/2^-, 1/2$	39.245 (39.110)	-2.467 (-2.529)	3.57 ± 0.15 $\text{fm}^{-1/2}$	3.44 $\text{fm}^{-1/2}$	-7.25 (-7.639)	th.results [63] $l = 1, J_n = 1/2$ $1.652 \text{ fm}^{-1/2}$ $l = 1, J_n = 3/2$ $1.890 \text{ fm}^{-1/2}$	$l = 1, J_n = 1/2$ $-1.618 \text{ fm}^{-1/2}$ $l = 1, J_n = 3/2$ $1.317 \text{ fm}^{-1/2}$
$1/2^-, 1/2$	38.768 (38.279)	-1.98 (-1.69)	3.0 ± 0.15 $\text{fm}^{-1/2}$	2.95 $\text{fm}^{-1/2}$	-6.77 (-6.808)	th.results [63] $l = 1, J_n = 1/2$ $-0.540 \text{ fm}^{-1/2}$ $l = 1, J_n = 3/2$ $-2.540 \text{ fm}^{-1/2}$	$l = 1, J_n = 1/2$ $-0.531 \text{ fm}^{-1/2}$ $l = 1, J_n = 3/2$ $1.979 \text{ fm}^{-1/2}$
$1/2^+, 1/2$	32.804 (28.921)	3.984 (7.66)	3.15 MeV	7.4 MeV	-0.81 (2.55)	$\Gamma(E = 1eV)$ 0.29 keV	$l = 0, S = 1/2$ $\Gamma(E = 1eV)$ 0.54 keV

 Table 3: Asymptotic characteristics of ${}^7\text{Li}$ for ${}^4\text{He}+{}^3\text{H}$ and ${}^6\text{Li}+n$ channels for high-excited negative parity states.

J^π, T	$E_{exp.}(E_{th.})$ MeV	$E_{\alpha+t}^{exp.}$ ($E_{\alpha+t}^{th.}$) MeV	$\Gamma_\alpha(\text{ANC})$ [61, 62]	$\Gamma_\alpha(\text{ANC})$ th.	$E_n^{exp.}$ ($E_n^{th.}$) MeV	$\Gamma_n(\text{ANC})$ [55, 63]	$\Gamma_n(\text{ANC})$ th.
$7/2^-, 1/2$	34.593 (34.409)	2.195 (2.172)	69 keV	65 keV	-2.59 (-2.938)	—	$l = 3, S = 1/2$ $0.013 \text{ fm}^{-1/2}$
$5/2^-, 1/2$	32.641 (31.610)	4.147 (4.971)	tot.: 918 keV	564 keV	-0.65 (-0.139)	—	$l = 1, S = 3/2$ $0.199 \text{ fm}^{-1/2}$
$5/2^-, 1/2$	31.791 (30.816)	4.997 (5.765)	22.9 keV	797 keV	0.2 (0.655)	57.7 keV	$l = 1, S = 3/2$ 53 keV
$3/2^-, 1/2$	30.495 (28.175)	6.293 (8.406)	tot.: 4.7 MeV	873 keV	1.5 (3.296)	0.867 MeV	$l = 1, S = 1/2$ 88 keV $l = 1, S = 3/2$ 1.0 MeV
$1/2^-, 1/2$	30.155 (27.280)	6.633 (9.301)	tot.: 2.7 MeV	282 keV	1.84 (4.191)	—	$l = 1, S = 1/2$ 230 keV $l = 1, S = 3/2$ 1.0 MeV
$7/2^-, 1/2$	29.675 (28.489)	7.133 (8.092)	tot.: 437 keV	453 keV	2.32 (2.982)	—	$l = 3, S = 1/2$ 0.72 keV
$3/2^-, 1/2$	— (27.047)	— (9.60)	—	1.25 MeV	— (4.424)	—	$l = 1, S = 1/2$ 785 keV

 Table 4: Asymptotic characteristics of high-excited states of ${}^7\text{Li}$ for ${}^6\text{He}(\text{gr.})+p$ and ${}^6\text{Li}(E^*=3.562 \text{ MeV}, T=1)+n$ channels.

J^π, T	$E_{exp.}(E_{th.})$ MeV	$E_{He+p}^{exp.}$ ($E_{He+p}^{th.}$) MeV	Γ_{tot} [61]	SF_{He+p}	Γ_{He+p} (ANC) th.	$E_{Li+n}^{exp.}$ ($E_{Li+n}^{th.}$) MeV	SF_{Li+n}	Γ_{Li+n} (ANC)
$1/2^-, 1/2$	30.155 (27.280)	-0.885 (1.538)	—	0.1465	0.343 $\text{fm}^{-1/2}$	-1.727 (0.638)	0.0453	0.259 $\text{fm}^{-1/2}$
$3/2^-, 3/2$	28.005 (27.247)	1.265 (1.571)	260 keV	0.1638	111 keV	0.433 (0.671)	0.3770	117 keV

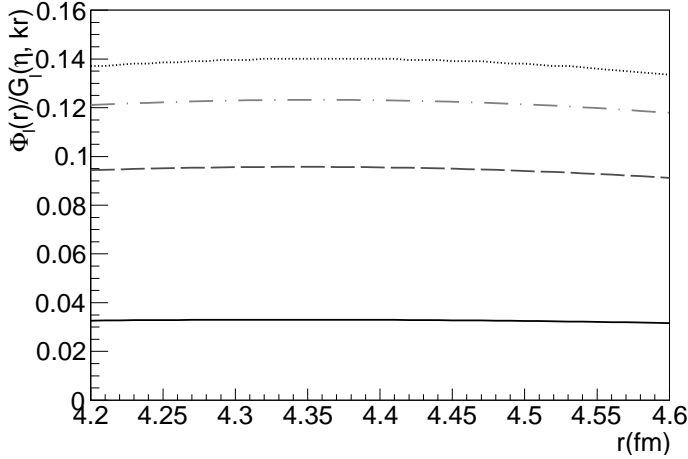


Figure 5: The ratio of the CFF and the irregular Coulomb function ($\Phi_1(r)/G_1(\eta, kr)$) in the region of the matching point for the $7/2_1^-$ (solid line), $5/2_1^-$ (dashed line), and $5/2_2^-$ (dashed-dotted line) states and the ratio of the CFF $\Phi_1(r)$ and $(G_1^2(\eta, kr) + F_1^2(\eta, kr))^{1/2}$ (dotted line) for high-excited $7/2_2^-$ state.

The ratios of CFFs and irregular asymptotic solutions for $7/2_1^-$, $5/2_1^-$ and $5/2_2^-$ states are also stable (see Fig. 5). They are located in the sub-barrier region and satisfy the condition $F_1(\eta, kr) \ll G_1(\eta, kr)$ and, thus, the condition of equality of the logarithmic derivatives of CFFs and irregular solutions is valid.

In the case of highly-excited state $7/2_2^-$ the inequality (16) is not satisfied, so the conventional R -matrix theory (21) is used. The ratio of CFF of the ${}^4\text{He} + {}^3\text{H}$ channel and $(G_1^2(\eta, kr) + F_1^2(\eta, kr))^{1/2}$ according to Fig. 5 is stable. This example shows that our method remains applicable even for high-excited states.

In our previous paper [41] it was shown that $7/2_1^-$ state is strongly clustered. Its calculated decay width is in a very good agreement with the experimental value as it is shown in Tab. 3. In Ref. [61], this value is presented as an alternative to a commonly accepted value 93 keV [62]. Taking into account a high stability of the calculations performed, we consider the result as a serious argument in favor of the value shown in [61]. In contrast to the successful description of the asymptotic characteristics of three lowest levels, the width of the $5/2_2^-$ level calculated with the Daejeon16 potential is strongly inconsistent with the experimental value though the aggregate decay width of two $5/2_2^-$ levels is reproduced more or less well. We guess that this discrepancy is due to the fact that these states are overlapped. Indeed, the energy distance (~ 800 keV) between them is smaller than the aggregate decay width observed in the experiments. The small distance makes the WFs of the overlapping states to be sensitive to a small variation of the parameters of the used potential. In the discussed case the large overestimation of $5/2_2^-$ state decay width is possibly determined by the contribution of the components with the spin $S = 1/2$. The excess of these components obtained in the calculations for this state and, correspondingly, their deficit in the $5/2_1^-$ state indicate some features of the description of spin-dependent forces by the potential in use. It is clear that any calculation can hardly reproduce the statistical weights of small components with a proper accuracy; meanwhile, the presence of such components with

the spin $S = 1/2$ determines the asymptotic characteristics of the ${}^4\text{He} + {}^3\text{H}$ channel for this state. It is interesting to note that problem of reproducing the energy gap between $3/2_1^-$ and $1/2_1^-$ states in the computations performed with the use of Daejeon16 potential is obviously associated with the spin-dependent part of it too. Perhaps there are other effects originated by overlapping of $5/2_{1,2}^-$ resonance states.

The decay widths of ${}^4\text{He} + {}^3\text{H}$ channel are calculated also for other highly-excited states such as $3/2_2^-$, $3/2_3^-$ and $1/2_2^-$. The results do not contradict much with known data, especially bearing in a mind that the widths of this highly-excited states couldn't be extracted with a high accuracy from experimental data.

The asymptotic characteristics of the discussed states are calculated also for other decay channels. For ${}^6\text{Li} + n$ channel our results demonstrate a good agreement with known decay widths for $5/2_2^-$ and even for exotic $1/2^+$ state. In the case of $5/2_2^-$ it is even more surprising since as it is shown above the decay width for ${}^4\text{He} + {}^3\text{H}$ is overestimated. From this it follows that possible defects in the used NN-potential does not strongly affect the WF as a whole but only some number of its components. It should be mentioned that the presented method is applicable even for calculations of the asymptotic characteristics of neutron s -wave channels as it is shown by the example of $1/2^+$ state. For other states not much information is known. So the results just presented are the most complete for neutron decay channel of ${}^7\text{Li}$ nucleus.

The discussed method is also used for channels containing exotic subsystems (isobar analogues ${}^6\text{He}$ (ground) and ${}^6\text{Li}$ ($E^* = 3.562$ MeV, $T = 1$)). The results related to only two states $1/2_2^-$ and $3/2$ ($T=3/2$) are presented. It is because only they have significant values of the spectroscopic factors for these channels and only they are located in the near-threshold region. Solely the total width of $3/2$ ($T=3/2$) state (≈ 260 keV) is known from the experimental data and the calculated value agree with it perfectly since the aggregate two-channel decay width of this state is 228 keV. For sub-threshold state $1/2_2^-$ neither experimental nor other theoretical data concerning these two channels are known. Nevertheless it is obvious that eventually the method showed its high reliability and wide applicability in this example ones more.

The main results of this work are the following.

- I. Within the framework of outgrows of the Cluster Channel Orthogonal Functions Method an ab initio scheme for computing the asymptotic characteristics of nuclear states, namely the asymptotic normalization coefficients of bound states and partial decay widths of resonances is designed. This method is founded on the conventional NCSM and the projection procedure of WFs of the model onto the cluster channel functions. At the same time not only NCSM WFs but other ones obtained in an ab initio approach and representable in the form of shell-model expansion can be exploited in the approach.
- II. This scheme allows one to obtain simultaneously the asymptotic characteristics of arbitrary two-fragment real and virtual decay channels of all known states of light nuclei.
- III. The asymptotic characteristics of the bound and resonant states of ${}^7\text{Li}$ are calculated for all two-body decay channels of

interest. Good agreement with the experimental data is achieved not only for the dominating decay channels, but also for channels with exotic subsystems. The results of the computations demonstrate prospects of the method to obtain experimentally unknown ANC's of bound states and partial decay widths of resonant states of light nuclei.

IV. It is demonstrated that the approach may be promising as an additional test on NN-interaction used as an input.

V. The performed calculations of the asymptotic characteristics of all low-lying states of light nuclei will allow, in the short term, to achieve a keen insight into delicate microscopic effects when calculating the cross sections of resonant and peripheral nuclear reactions induced by collisions of light nuclei.

VI. The authors believe that the current work may turn out to be a step on the way to creation of the theoretical nuclear spectroscopy which allows one to reproduce and predict all observables characterizing light nuclei.

References

- [1] C. Stump, J. Braun, R. Roth, Phys. Rev. C **93** (2016) 021301.
- [2] P. Navratil, S. Quaglioni, I. Stetcu, B. Barrett, J. Phys. G: Nucl. Part. Phys. **36** (2009) 083101.
- [3] S.E. Koonin, D.J. Deand, K. Langanke, Phys. Reports **278** (1997) 1.
- [4] T. Dytrych, K. D. Sviratcheva, C. Bahri, J. P. Draayer, and J. P. Vary, Phys. Rev. C **76** (2007) 014315.
- [5] A. C. Dreyfuss, K. D. Launey, T. Dytrych, J. P. Draayer, and C. Bahri, Phys. Lett. B **727** (2013) 511 .
- [6] G. Papadimitriou, J. Rotureau, N. Michel, M.P. Loszajczak, B.R. Barrett, Phys. Rev. C **88** (2013) 044318.
- [7] I.J. Shin, Y. Kim, P. Maris, J.P. Vary, C. Forssen, J. Rotureau, N. Michel, J. Phys. G: Nucl. Part. Phys. **44** (2017) 075103.
- [8] S.C. Pieper, R.B. Wiringa, Ann. Rev. Nucl. Part. Sci. **51** (2001) 53.
- [9] B.S. Pudliner et al, Phys. Rev. C **56** (1997) 1720.
- [10] R.B. Wiringa et al., Phys. Rev. C **62** (2000) 014001.
- [11] H. Kummela, K.H. Luhrmann, J. Zabolitzky, Phys. Rep. **36** (1978) 1.
- [12] M.G. Endres, D.B. Kaplan, J.-W. Lee, A.N. Nicholson, Phys. Rev. A **84** (2011) 043644.
- [13] M.G. Endres, D.B. Kaplan, J.-W. Lee, A.N. Nicholson, Phys.Rev. A **87** (2013) 023615.
- [14] K. Orginos, A. Parreno, M.J. Savage, S.R. Beane, E. Chang, W. Detmold, Phys. Rev. D **92** (2015) 114512.
- [15] A.M. Shirokov, I.J. Shin, Y. Kim, M. Sosonkina, P. Maris, J.P. Vary, Phys. Lett. B **761** (2016) 87.
- [16] R. Machleidt, D.R. Entem, Phys. Rep. **503** (2011) 1.
- [17] D.R. Entem, R. Machleidt, Phys. Rev. C **66** (2002) 014002.
- [18] A.M. Shirokov, J.P. Vary, A.I. Mazur, T.A. Weber, Phys. Lett. B **644** (2007) 33.
- [19] J.A. Wheeler, Phys. Rev. **52** (1937) 1107.
- [20] K. Wildermuth, Y.C. Tang *A Unified Theory of the Nucleus* (Braunschweig: Vieweg, 1977).
- [21] G.F. Filippov, I.P. Okhrimenko, Phys. Atom. Nucl. **32** (1980) 480.
- [22] A.S. Solov'yev, S.Y. Igashov, Phys. Rev. C **96** (2017) 064605.
- [23] H. Horiuchi, Prog. Theor. Phys. Suppl. **62** (1977) 90.
- [24] A. Adahchour, P. Descouvemont, Nucl. Phys. A **813** (2008) 252.
- [25] P. Descouvemont, D. Baye, Phys. Lett. B **505** (2001) 71.
- [26] K. Arai, P. Descouvemont, D. Baye, W. Catford, Phys. Rev. C **68** (2003) 014310.
- [27] A. Tohsaki, H. Horiuchi, P. Schuck, G. Roepke, Phys. Rev. Lett. **87** (2001) 192501.
- [28] Y. Kanada-En'yo, H.Horiuchi, Prog. Theor. Phys. Suppl. **142** (2001) 205.
- [29] S. Quaglioni, P. Navratil, Phys. Rev. C **79** (2009) 044606.
- [30] S. Baroni, P. Navratil, S. Quaglioni, Phys. Rev. C **87** (2013) 034326.
- [31] P. Navratil, S. Quaglioni, G. Hupin, C. Romero-Redondo, A. Calci, Phys. Scr. **91** (2016) 053002.
- [32] A. Bonaccorso, F. Cappuzzello, et al., Phys. Rev. C **100** (2019) 024617.
- [33] M. Vorabbi, P. Navratil, et al., Phys. Rev. C **100** (2019) 024304.
- [34] T. Neff, H. Feldmeier, Int. J. Mod. Phys. E **17** (2008) 2005.
- [35] T. Neff, Phys. Rev. Lett. **106** (2011) 042502.
- [36] T. Neff, H. Feldmeier, JPS Conf. Proc. **23** (2018) 012029.
- [37] D.M. Rodkin, Yu.M. Tchuvil'sky, J. Phys.: Conf. Ser. **966** (2018) 012022.
- [38] D.M. Rodkin, Yu.M. Tchuvil'sky, Phys. Lett. B **788** (2019) 238.
- [39] K. Kravvaris, A. Volya, Phys. Rev. Lett. **119** (2017) 062501.
- [40] A.M. Shirokov, A.I. Mazur, I.A. Mazur, J.P. Vary, Phys. Rev. C **94** (2016) 064320.
- [41] D.M. Rodkin, Yu.M. Tchuvil'sky, JETP Lett. **108** (2018) 429.
- [42] Yu.F. Smirnov, Nucl. Phys. **39** (1962) 346.
- [43] O.F. Nemets, V.G. Neudachin, A.E. Rudchik, Yu.F. Smirnov, Yu.M. Tchuvil'sky, *Nuclear Clusters in Atomic Nuclei and Multinucleon Transfer Reactions* (Naukova Dumka, Kiev, 1988).
- [44] Yu.F. Smirnov, Yu.M. Tchuvil'sky, Phys. Rev. C **15** (1977) 84.
- [45] Yu.F. Smirnov, Yu.M. Tchuvil'sky, Czech. J. Phys. **33** (1983) 215.
- [46] Yu.M. Tchuvil'sky, W.W. Kurowsky, A.A. Sakharuk, V.G. Neudatchin, Phys. Rev. C **51** (1995) 784.
- [47] T. Fliessbach, H.J. Mang, Nucl. Phys. A **263** (1976) 75.
- [48] R.G. Lovas, R.J. Liotta, A. Insolia, K. Varga, D.E. Delion, Phys. Rep. **294** (1998) 265.
- [49] S.G. Kadmsky, S.D. Kurgalin, Yu.M. Tchuvil'sky, Phys. Part. Nucl. **38** (2007) 699.
- [50] A. Volya, and Yu. M. Tchuvil'sky, Phys. Rev. C **91** (2015) 044319.
- [51] A. Volya, and Yu. M. Tchuvil'sky, Phys. At. Nucl. **79** (2016) 772.
- [52] S.G. Kadmsky, V.I. Furman, *Alpha-Decay and Related Nuclear Reactions* (Energoatomizdat, Moscow, 1985) [in Russian].
- [53] L.D. Blokhintsev, I. Borbey, E.I. Dolinskii, Sov. J. Part. Nucl. **8** (1977) 485.
- [54] S.B. Igamov, R. Yarmukhamedov, Nucl. Phys. A **781** (2007) 247.
- [55] S.I. Sukhoruchkin, et al., *Low Energy Neutron Physics* (Springer, 1998).
- [56] A.M. Mukhamedzhanov, et al., Phys. Rev. C **59** (1999) 6.
- [57] D.R. Entem, R. Machleidt, Phys. Rev. C **68** (2003) 041001.
- [58] S.K. Bogner, R.J. Furnstahl, R.J. Perry, Phys. Rev. C **75** (2007) 061001.
- [59] C.W. Johnson, W.E. Ormand, et al., (2018) arXiv:1801.08432 [physics.comp-ph].
- [60] P. Descouvemont, D. Baye, Progr. Rep. Phys. **77** (2010) 036301.
- [61] D.R. Tilley, C.M. Cheves, J.L. Godwina, G.M. Haled, H.M. Hofmann, J.H. Kelleys, C.G. Sheua, H.R. Weller, Nucl. Phys. A **708** (2002) 3.
- [62] R.B. Firestone, et al., *Table of isotopes*, (Wiley-Interscience, 1996).
- [63] K.M. Nollett, R.B. Wiringa, Phys. Rev. C **83** (2011) 041001(R).